Structure-Related Behavior of Hybrid Organic–Inorganic Materials Prepared in Different Synthesis Conditions from Zr-Based NBBs and 3-Methacryloxypropyl Trimethoxysilane

R. Di Maggio, E. Callone, F. Girardi, S. Dirè

Dipartimento di Ingegneria dei Materiali e Tecnologie Industriali, University of Trento, Trento, Italia

Received 10 December 2010; accepted 10 September 2011
DOI 10.1002/app.36255
Published online 17 January 2012 in Wiley Online Library (wileyonlinelibrary.com).

ABSTRACT: The copolymerization of zirconium oxo-clusters (Zr12) with 3-methacryloxypropyl (trimethoxy)silane (MPTMS), using a Si/Zr molar ratio of 4, was investigated. The hybrid samples were prepared both with and without organosilane prehydrolysis. Differential scanning calorimetry (DSC), multinuclear liquid, and solid state NMR analyses and Fourier transform infrared (FTIR) spectroscopy were used to characterize the hybrid materials and study the influence of synthesis conditions on condensation and polymerization. The degree of condensation (DOC) of the silsesquioxane network and the polymerization yield are generally high. However, the organosilane prehydrolysis step leads to the reduction of the extent of phase interaction, thus favoring the phase separation between silica-zirconia-based domains. Dynamic mechanical spectroscopy (DMS) analyses were performed on the hybrid polymers obtained by means of the two synthetic pathways. The sample prepared without the organosilane prehydrolysis step presents a higher glass transition temperature (T_g) than the one with silane prehydrolysis. By heating above the T_g, the samples retain shape and size, due to the lack of viscous flow. © 2012 Wiley Periodicals, Inc. J Appl Polym Sci 125: 1713–1723, 2012

Key words: *I/O* hybrid; zirconium oxo-cluster; vinylacetic acid; 3-methacryloxypropyl trimethoxysilane; glass transition temperature

INTRODUCTION

In recent years, the synthesis of hybrid inorganic–organic polymers and their potential applications from catalysis to optics have been amply studied with a view to preparing materials with enhanced mechanical, magnetic and thermal properties.[1–9] The final architecture can be controlled and a homogeneous dispersion of the inorganic components in the organic matrix can be achieved by means of well-defined reaction steps from molecular level onwards. The sol–gel process is a powerful synthetic route for producing oxide systems and embedding organic components in the oxide network, but heterogeneous materials can be obtained if hydrolysis and precursor condensation rates are not fully under control. The size of the organic and inorganic domains is a major concern: the larger the size, the greater the heterogeneity of the hybrid material, with severely detrimental effects for some applications. This aspect has to be considered especially carefully when the main goal is to prepare multi-component hybrid materials. One recent approach involved making prehydrolyzed silanes (3-methacryloxypropyl triethoxysilane [MPTES], 3-methacryloxymethyl triethoxysilane [MMTES] and methacryloxypropyl trimethoxysilane [MPTMS]) react with transition metal oxo-clusters $M_4O_2(OMc)_{12}$ (M = Zr, Ti, Hf; Mc = methacrylate) (Zr4), then copolymerizing the methacrylate groups linked to the siloxane network and those capping the metal oxo-clusters.[10–12] The aim of these previous studies was to investigate the influence of the hybrid materials' molecular composition on the final structure of the resulting binary oxide phases MO_2-SiO_2 (with M = Zr, Ti, Hf), without devoting attention to the polymerization process.[10–12] This approach has the merit of using a well-defined, single-size metal oxide core and several studies conducted by Schubert et al. on carboxylate surface-functionalized zirconium oxo-clusters have shown that this class of compounds possesses various shapes, depending on the nature of the carboxylic acid and the ratio of metal alkoxide to carboxylic acid.[13–16]

The copolymerization of vinyl trimethoxysilane (VTMS) and vinyl-acetate-substituted zirconium oxo-

Correspondence to: R. Di Maggio (rosa.dimaggio@unitn.it).

Contract grant sponsors: PAT "CENACOLI", MIUR (PRIN 2009).

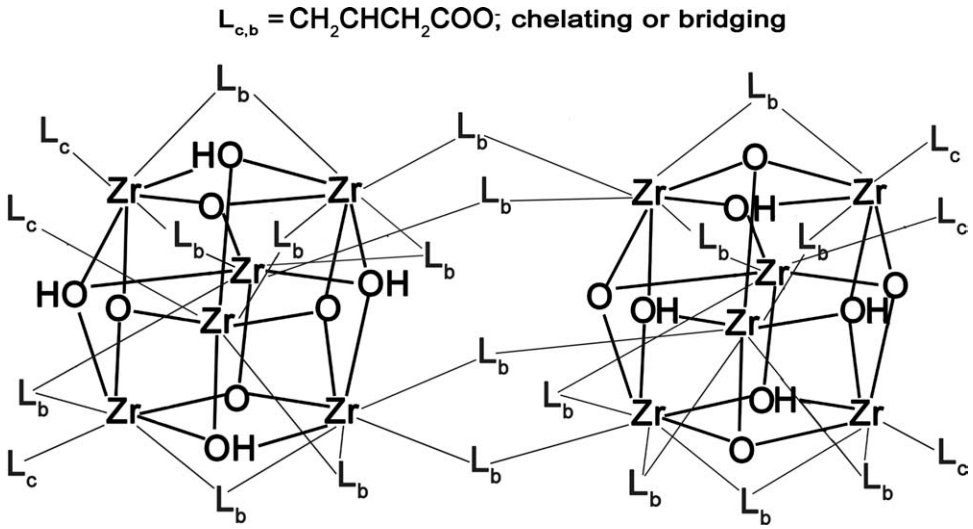

Scheme 1 Structure of the cluster.

clusters (Zr12) to produce inorganic-organic hybrid polymers for coating or massive applications from low to high temperatures has recently been reported.[17,18] These clusters with the molecular formula $[Zr_6O_4(OH)_4(OOCCH_2CH{=}CH_2)_{12}(n\text{-}PrOH)]_2 \cdot 4(CH_2{=}CHCH_2COOH)$ (Zr12) were described by Schubert et al.[13–18] as dimers containing six zirconium atoms (Zr6) linked by bridging carboxylate groups forming the cluster Zr12, which formula is shown in Scheme 1.

The Zr12 crystals are colorless and do not dissolve in water, while they are soluble in various organic solvents, such as toluene, THF, and ethyl acetate.[19–21] The Differential Scanning Calorimetry (DSC) study demonstrated that these oxo-clusters decompose endothermally on heating, whereas they can give rise to an exothermal polymerization process in the presence of a thermal initiator, such as benzoyl peroxide (BPO). The structural and mechanical characteristics of bulk hybrid materials prepared by mixing VTMS and Zr12 depend on whether a prehydrolyzed VTMS solution is used or the organosilane is added without the prehydrolysis step.[19,20] The preparation of hybrid materials from VTMS exploits both methoxide group hydrolysis/condensation to form the silica network and vinyl group polymerization to form the organic backbone. It has been demonstrated in the literature that the sequence of the two processes is important.[22–24] If the hydrolysis/condensation step takes place before polymerization, the growth of ample silica domains is favored and the vinyl groups are less available for radical polymerization. Vice versa, if polymerization occurs first, the polymer chains are longer and the silica domains remain small.[22–24]

On the basis of the literature[22–26] on vinyl and acrylate modified silanes and carboxylate-functionalized metal oxo-clusters, it appears clear that many different reactions take place, during hybrids formation the competition among them leads to different structure-related properties. In order to manage the networks formation, the following chemical processes for the inorganic network development from organosilanes (eqs. 1 and 2) should be taken into account:

$$\text{Si—OR} + \text{H}_2\text{O} \rightleftharpoons \text{Si—OH} + \text{R—OH} \qquad (\text{R} = \text{Me}) \tag{1}$$

$$\text{Si—OH} + \text{X—OSi} \rightleftharpoons \text{Si—O—Si} + \text{X—OH} \qquad (\text{X} = \text{H or R}) \tag{2}$$

The hydrolysis reaction (eq. 1) takes place upon water addition leading to the formation of silanols and the condensation step (eq. 2) can involve both hydrolyzed and not hydrolyzed units. Thus, condensation can take place also with very small amounts of water, like in the presence of moisture, or can be promoted by thermal cleavage of the alkoxide groups (eq. 3).

$$\text{Si—OR} + \text{RO—Si} \xrightarrow{\Delta} \text{Si—O—Si} + \text{R—O—R} \tag{3}$$

Depending on the conditions, the condensation of the inorganic network can lead to ladder-like polymers, cycles and linear species.[27]

In hybrid systems, the polymerizable organic groups undergo mainly the radical polymerization, particularly in the presence of suitable thermal or photo-initiators (Scheme 2).

The preparation of hybrids from organosilanes and metal oxo-clusters should consider also the possibility of copolymerization, which can be promoted by interactions between phases (Schemes 3, 4, and 5).

Scheme 2 Radical polymerization of vinyl or acrylate silane.

A compliant network, such as in the case of low degree of inorganic network condensation or the formation of flexible and mobile siloxane chains, favors the radical copolymerization (Scheme 3). Moreover, it can depend also on the interactions between the silane organic functions and the metal sites in the oxoclusters, acting as coordination centers (Scheme 4), or the H bonding interaction between silanols and acrylate functions (Scheme 5).[28]

According to the extent of reactions 1-3, the network can develop different size silica domains. Performing hydrolysis-condensation at first (eqs. 1 and 2) leads to large silica domains, and the organic polymerization (Schemes 2 and 3) could be inhibited by the lack of flexibility in the network, leading to stiff and fragile networks. On the contrary, when organic polymerization (Schemes 2 and 3) is carried out at first, only small silica domains can be obtained and rubbery samples can be produced. The formation of small silica domains can also favor homo and copolymerization (Schemes 4 and 5) and the increase in phase interaction can lead to rigid samples.

In this article, we investigated the final structural features of hybrid materials prepared using MPTMS and $[Zr_6O_4(OH)_4(OOCCH_2CH{=}CH_2)_{12}(n\text{-}PrOH)]_2 \cdot 4(CH_2{=}CHCH_2COOH)$ (Zr12). It is reasonable to expect that this composition will lead to different results with respect to those obtained in the previous study on VTMS/Zr12. We focused on the polymerization process to verify whether homo-polymerization/co-polymerization processes could take place between the methacrylate and the vinyl groups, providing homogenous polymers. Moreover, the aim of our study was also to evaluate the effect of MPTMS prehydrolysis on radical polymerization process and final properties of the hybrid polymer.

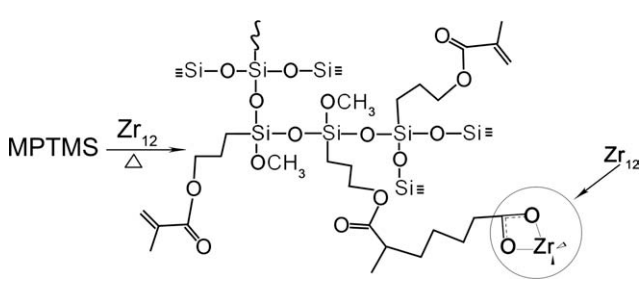

Scheme 3 Radical copolymerization of vinyl and acrylate groups of zirconium oxo-cluster and organosilane.

EXPERIMENTAL PART

Materials

The reagents were purchased by Aldrich and used as received, without further purification. The synthesis of Zr12 has been described elsewhere.[17,18]

Synthesis of Zr12/MPTMS/BPO

The Zr12 crystals were dissolved in tetrahydrofuran (THF) (0.06 M) and 3-methacryloxypropyl (trimethoxy)silane (MPTMS) was added to the solution under stirring, in air at room temperature. A solution was prepared with a Zr : Si molar ratio of 1 : 4. The weighed amount of benzoyl peroxide (BPO) corresponding to 0.6% of the total mass (MPTMS and Zr12) was added to the mixture. After 24 h, the solution was concentrated to dryness under a reduced pressure and the xerogels obtained, labeled Zr12/MPTMS/BPO, were thermally cured at 95°C for 5 h and at 130°C for 1.5 h. Samples without BPO were also prepared and labeled Zr12/MPTMS.

For the sake of comparison, a sample labeled MPTMS/BPO was prepared without the addition of Zr12 by dissolving MPTMS and BPO (0.6 wt % of MPTMS) in THF (0.4 M). The pure MPTMS precursor was also analyzed without thermal initiator.

Synthesis of Zr12/MPTMS/H_2O/BPO

Hybrid samples were also prepared with a prehydrolysis step. The silane was dissolved in THF at a concentration of 0.4 M and reacted with acidic water

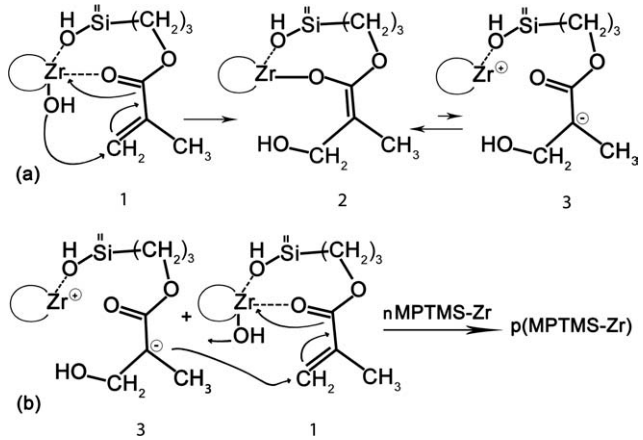

Scheme 4 Zirconium activation of MPTMS polymerization.

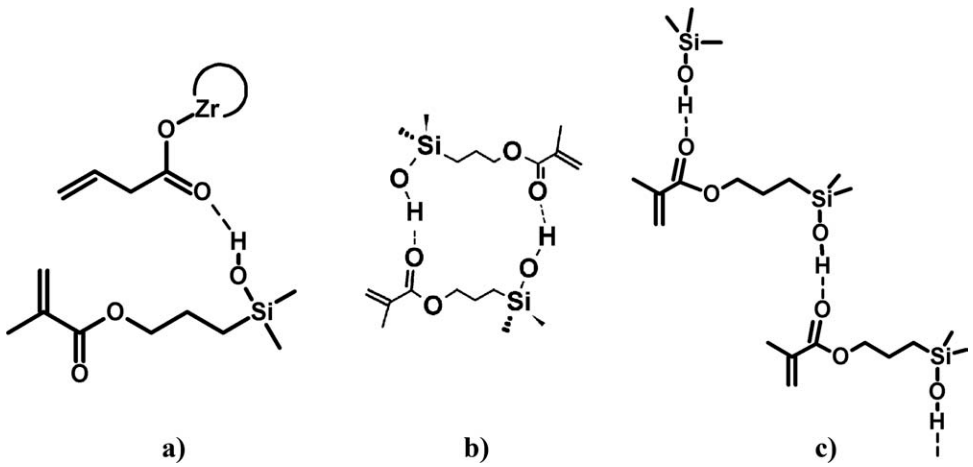

Scheme 5 Possible hydrogen bonding between hydroxyl and carboxylic groups.

(HCl) with a Si : H_2O molar ratio of 1 : 3 [29]. Zr12 and BPO were then added to the mixture and the hybrid xerogels were synthesized as described above. A sample labeled MPTMS/H_2O/BPO was prepared with MPTMS alone, using the above-mentioned synthesis conditions. The same samples without BPO were also prepared (Zr12/MPTMS/H2O and MPTMS/H_2O).

Measurement

Differential scanning calorimetry (DSC) analyses were performed with a DSC92 SETARAM, in N_2 with a heating rate of 10°C/min.

Dynamic mechanical spectroscopy (DMS) was performed in shear mode on cured hybrid materials with a cylindrical shape with planar and parallel faces 12 mm^2 in area and 3.5 mm thick, using a Seiko DMS 6100 instrument at a frequency of 1 Hz, with a displacement of 0.005 mm in the direction of the diameter. The test was performed in air, applying 1000 mN as the starting force, with a heating rate of 2°C min^{-1} up to 300°C. The shear storage modulus (G'), loss modulus (G'') and tan δ were measured. The glass transition temperature (Tg) was measured by recording the maximum loss modulus curve temperature. The DMS analysis was only performed for polymerized MPTMS without prehydrolysis, in compression mode and using the same instrumental conditions.

Fourier Transform InfraRed (FTIR) spectra were recorded in transmission mode in the range of 4000–400 cm^{-1} on KBr pellets (64 scans and 2 cm^{-1} resolution), using a Thermo Optics Avatar 330 FTIR instrument.

Solid-state Nuclear Magnetic Resonance (NMR) analyses were conducted with a Bruker 400WB instrument applying a carrier frequency of 400.13 MHz (^1H). One dimensional (1D) experiments were based on single pulse sequences under the following conditions: ^{29}Si at 79.50 MHz with π/2 3.6 μs at −2 dB, proton decoupling power −4.2 dB for 4.9 μs and 20-s delay time, 2000 scans; ^{13}C at 100.07 MHz, π/2 2.8 μs at −0.5 dB, 6.0 μs decoupling pulse and 10-s delay time, 300 scans. Samples were packed in 4 mm-zirconia rotors, which were spun at 6.5 kHz under air flow.

The classical T^n notation is used to represent three functional silicon units, where n is the number of oxo-bridges. Throughout the text, numbers according to Scheme 6 identify the carbon atoms.

RESULTS

Polymerization process

Polymer samples were prepared as explained in the experimental part, with and without prehydrolysis and with and without the thermal initiator.

A basic study on the thermal polymerization of neat MPTMS was undertaken in order to assess its ability to polymerize under different conditions (MPTMS systems), followed by the characterization of the hybrid materials obtained with Zr12 addition (Zr12/MPTMS systems). All these systems were studied with and without the addition of BPO.

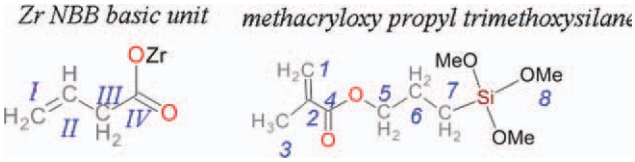

Scheme 6 Structural elucidation of the components (the numbers refer to different carbon atoms). [Color figure can be viewed in the online issue, which is available at wileyonlinelibrary.com.]

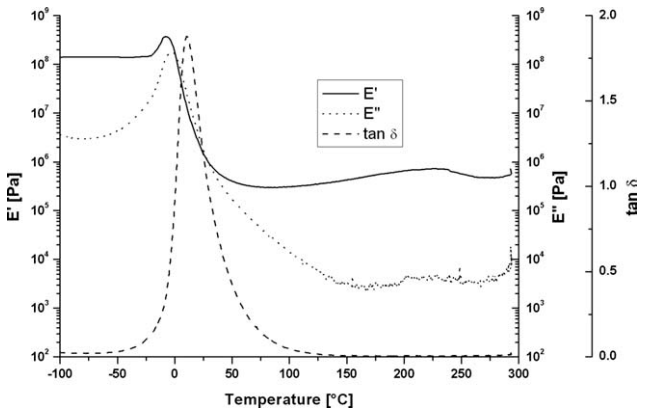

Figure 1 E', E'', and tan d vs. temperature of MPTMS/BPO sample polymerised at 95°C.

MPTMS systems

The DSC trace recorded in N_2 on neat MPTMS from room temperature up to 200°C showed no thermal phenomena; at the end of the analysis, a mass loss of about 18% was measured, which can be attributed mainly to the precursor evaporation.

The addition of both BPO and/or H_2O the thermal initiator modifies the thermal behavior of the pure MPTMS precursor.

In the DSC curve of MPTMS/BPO a large exothermal peak appeared due to polymerization (ΔH = 191 J/g, Δm = 4%, T_{onset} = 94°C and T_{max} = 138°C). On the basis of the DSC analysis, a temperature of 95°C was chosen for isothermal polymerization and treatment for 1 h proved necessary to polymerize MPTMS/BPO. This sample had a rubbery behavior at room temperature, as confirmed by the DMS analysis shown in Figure 1. Indeed, the T_g measured at the maximum of the E'' curve was −2.6°C.

The sample MPTMS/H_2O underwent a mass loss of about 38% in the same temperature range of DSC analysis, with two endothermal peaks having maxima at 78°C and 100°C, attributable to parent alcohol and water release, respectively.

In the DSC curve of MPTMS/H_2O/BPO sample, the main phenomenon was endothermal, accompanied by a small exothermal polymerization peak at 134°C. The mass loss was about 40%. Upon thermal polymerization, this sample provides too fragile polymer, so no DMS analyses could be carried out on it.

Zr12/MPTMS systems

DSC analyses of Zr12/MPTMS/H_2O and Zr12/MPTMS were performed up to 200°C and the curves are shown in Figure 2(a,b), respectively. In both conditions, there was a small exothermal peak at 120°C and an intense polymerization peak at 177°C [Fig. 2(a)] and 145°C [Fig. 2(b)], accompanied by mass losses of 21% and 26%, respectively. To compare the thermal behavior of the Zr12/MPTMS samples with results previously obtained on a similar system with VTMS, the DSC traces of the Zr12/VTMS hybrids are shown in Figure 2(c,d). The DSC traces of the two hydrolyzed materials show an endothermal peak.

The polymer samples obtained without adding BPO were too brittle, so they were not further characterized.

Zr12/MPTMS/BPO systems

The Zr12/MPTMS/BPO sample showed a sharp peak at 115°C, related to the homo-polymerization of the methacrylate groups of MPTMS [Fig. 3(a)]. It is worth noting that, there was a much less intense peak at a higher temperature (142°C), mainly attributable to Zr12 homo-polymerization as previously observed [20]. The total polymerization heat was about 153 J/g, and the measured mass loss was 2.5%, which is probably due to the residual condensation at high temperature.[30–32] Samples prepared with a higher Zr : Si ratio (not presented here) showed broader polymerization peaks, as observed in a previous study on VTMS/Zr12/BPO systems.[20]

The Zr12/MPTMS/H_2O/BPO showed a very similar curve, shifted towards higher temperatures. The polymerization peak, centered at 118°C, and a smaller exothermal peak at 146°C were visible [Fig. 3(b)]. Both peaks appeared broader than in the previous sample; consequently, further copolymerization at a higher temperature cannot be excluded.

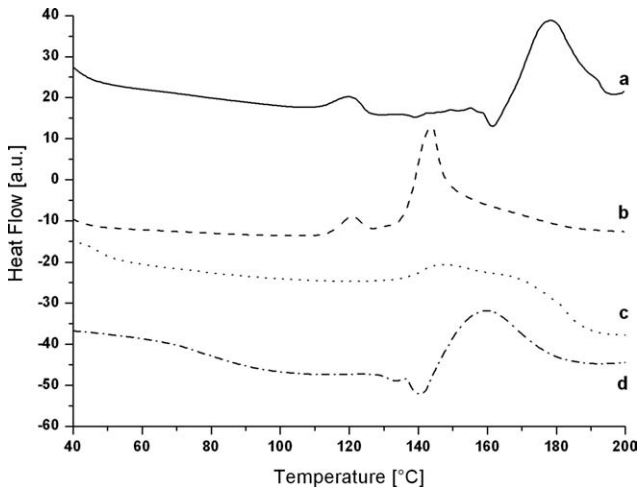

Figure 2 DSC curves of the four solutions having a Zr:Si molar ratio of 1 : 4: (a) Zr12/MPTMS/H_2O; (b) Zr12/MPTMS; (c) Zr12/VTMS/H_2O; (d) Zr12/VTMS.

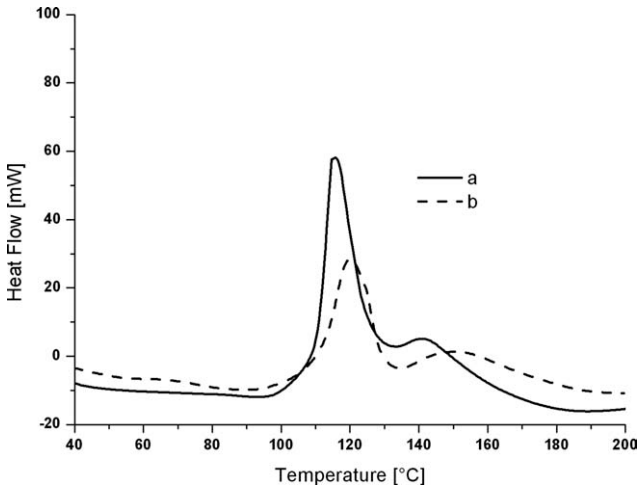

Figure 3 DSC curves of: (a) Zr12/MPTMS/BPO and (b) Zr12/MPTMS/H_2O/BPO (Zr:Si molar ratio 1 : 4).

The whole polymerization heat was 161 J/g, with about 11% of mass loss.

Several attempts were needed to optimize the production of bulk polymers suitable for studying their thermo-mechanical properties using dynamic-mechanical spectroscopy (DMS). Unlike other reports[11,12] on a polymerization temperature around 60°C and a curing step at 70°C of several hours, we chose to adopt a temperature of 95°C for the isothermal polymerization of bulk samples, based on the above-presented DSC results. At this temperature, polymerization takes 5 h to complete; the density of the polymers treated at 95°C appears similar for the two samples.

Thermo-mechanical measurements on Zr12/MPTMS/BPO hybrids

Whatever the synthesis conditions, the bulk samples polymerized at 95°C for 5 h were rather brittle. The polymerization conditions selected for this study nonetheless enabled the preparation of samples suitable for dynamic mechanical characterization, and more than two DMS scans were obtained on the samples. G' increased up to the T_g in the first DMS scan, then dropped. The G'' curve became progressively lower, with a small peak reaching a maximum of 140° for the sample that was prehydrolyzed, and 180°C for the sample that was not. Accordingly, the first peaks of the tan δ curves reached a maximum of 145°C and 193°C, respectively.

In the subsequent scans, G' and G'' showed constant values and no glass transition was detected. When the tan δ curve was plotted against the temperature, there were several peaks in the first DMS scan, while the curves recorded in those that followed were smoother and the peaks were less marked, indicative of a continuous increase in the density of the polymer network as the number of DMS scans increased.

The G' values measured at two different temperatures during each scan are given in Tables I and II. It is worth noting that, as the number of scans increased, the G' values rose, indicating that a progressively more rigid structural configuration was being reached as both organic polymerization and silica densification were being completed; this coincided with a loss of viscous behavior.

Tables I and II also show the mass loss recorded during each DMS scan, showing that the greatest loss was measured in the first scan for the prehydrolyzed sample, the mass of which remained almost constant in the subsequent scans (Table II).

The samples broke after a few DMS scans and turned brown due to a partial degradation of the organic moiety after heating up to 300°C.

Structural characterization

FTIR spectroscopy

The FTIR spectrum of MPTMS is characterized by the typical vibrations of the Si-OCH_3 group (ν_{CH3} 2840 cm^{-1}, δ_{CH3} 1455 cm^{-1}, ν_{SiOCH3} 1192 cm^{-1}, ν_{SiOCH3} 1072 cm^{-1}) and the signals relating to C=O ($\nu_{C=O}$ 1715 cm^{-1}, $\nu_{COunsat\alpha\beta ester}$ 1296 cm^{-1}, $\nu_{COunsat\alpha\beta ester}$1157 cm^{-1}) and C=C bonds ($\nu_{C=C}$ 1637 cm^{-1}, δ_{CH}1378 cm^{-1}, w_{CH2} 937 cm^{-1}) belonging to the methacrylate group. The Zr12 oxo-clusters have been characterized in detail in previous reports.[19,20] In the Zr12 FTIR spectrum, the C=O and C=C signals of the vinyl acetate groups appear at the same wave numbers as those due to the methacrylate group in MPTMS.

Figure 4 shows the FTIR spectra collected on the MPTMS/H_2O/BPO (trace a) and MPTMS/BPO (trace b) samples, polymerized at 95°C for 5 h. Very

TABLE I
The Zr12/MPTMS/BPO System: Δ*m*, *G*′, and *G*″ Measured at 40°C, *G*′, and *G*″ Measured at 250°C, tan δ Measured at 40°C and 250°C

	Δ*m*	*G*′ (40°C)	*G*″ (40°C)	*G*′ (250°C)	*G*″ (250°C)	tan δ (40°C)	tan δ (250°C)
1 scan	−9.98%	4.10×10^7	2.02×10^6	4.49×10^6	2.53×10^5	0.0495	0.0564
2 scan	−11.58%	5.99×10^7	2.43×10^6	6.00×10^7	1.47×10^6	0.0337	0.0245
3 scan	–	3.23×10^7	1.58×10^6	9.87×10^7	1.60×10^6	0.0491	0.0154

TABLE II
The Zr12/MPTMS/BPO/H_2O System: Δm, G', and G'' measured at 40°C, G', and G'' Measured at 250°C, tan δ Measured at 40°C and 250°C

	Δm	G' (40°C)	G'' (40°C)	G' (250°C)	G'' (250°C)	tan δ (40°C)	tan δ (250°C)
1 scan	−17.84%	3.9×10^7	2.61×10^6	1.68×10^5	3.89×10^4	0.0661	0.232
2 scan	−1.20%	4.84×10^7	1.65×10^6	5.50×10^7	1.11×10^6	0.0343	0.0205
3 scan	−0.65%	7.19×10^7	2.73×10^6	8.40×10^7	1.65×10^6	0.0382	0.0199
4 scan	−0.37%	3.351×10^7	1.61×10^6	5.99×10^7	1.36×10^6	0.0481	0.0243

small residual methoxy group signals are detectable in the spectrum of the prehydrolyzed sample [Fig. 4(a)] and a large siloxane band appears, generated by the peaks at 1167 (ladder-like polymer), 1109 (T_8OH_2 cages), 1060 (T_6OH_2), and 1011 (trimers) cm^{-1} overlapping.[33–36] The high intensity of the C=C related signals is worth noting. Though it is larger, the C=O signal appears in the same position as the MPTMS precursor. The FTIR results show an extended hydrolysis-condensation and a partial C=C polymerization.

On the other hand, the spectrum of the MPTMS/BPO polymer sample (trace b) highlights a considerable extent of C=C polymerization and a negligible extent of hydrolysis-condensation. Indeed, the methoxy-related signals appear intense and only the small peak at 1150 cm^{-1} accounts for the formation of siloxane bonds in a ladder-like polymer structure. Instead, very small residual C=C related signals are found together with the large shift in the C=O signal (15 cm^{-1}), which shows some signs of broadening.

The spectra of the Zr12/MPTMS/BPO samples with and without prehydrolysis are shown in Figure 4(c,d), respectively. The organosilane prehydrolysis (trace c) leads to very small residual methoxy group signals and the siloxane band is similar to the one in spectrum 4a. There are also signals at 3650 and 982 cm^{-1} due to some Si-OH groups. The low intensity of the C=C signals and the broadening of the C=O signal suggest a significant extent of C=C polymerization. The reduction in intensity and the broader bridging acetate signals at 1440 and 1577 cm^{-1}, when compared with the pristine Zr12 spectrum,[19,20] seem to indicate a change in Zr12 structure. The Zr12/MPTMS/BPO spectrum [Fig. 4(d)] shows a marked hydrolysis-condensation. On comparing traces d and b in Figure 4, this result is clearly apparent and suggests a promoter effect of Zr12. This last also affects siloxane oligomer formation: the siloxane band is the result of different signals, with intense peaks at 1170 (ladder-like polymers), 1036 (4-member open chains) and 1016 (trimers) cm^{-1} overlapping. There is probably less C=C polymerization than in the prehydrolyzed system (trace c). The reduction in intensity and the broader bridging acetate signals at 1440 and 1577 cm^{-1} appear more marked than in the prehydrolyzed hybrid.

^{29}Si NMR

^{29}Si NMR spectra account for the behavior of the inorganic part of the systems. First, some expected results emerge from the data in Table III. T^0 remains above 60% in the MPTMS/BPO sample, confirming that the thermal process has only a minor effect on condensation of Si-OMe bonds.[37] Adding water hydrolyses all the methoxy groups, favoring the inorganic matrix condensation; the silsesquioxane network is made of T^2 and T^3 species and the condensation exceeds 80%, as indicated by the degree of condensation (DOC),[38] calculated according to the following eq. (4) for a T-based network:

$$\mathrm{DOC} = \frac{T^1 + 2T^2 + 3T^3}{3(T^0 + T^1 + T^2 + T^3)} \cdot 100 \qquad (4)$$

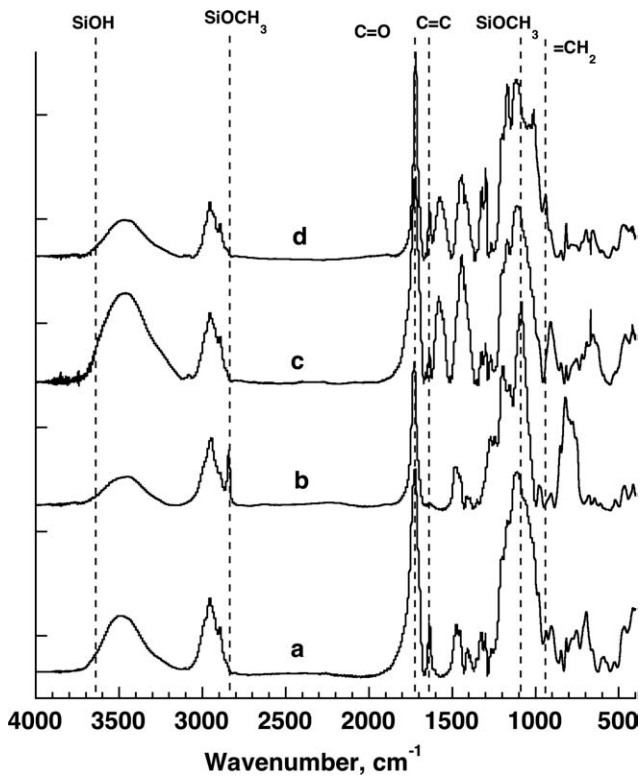

Figure 4 FTIR spectra of: (a) MPTMS/H_2O/BPO; (b) MPTMS/BPO; (c) Zr12/MPTMS/H_2O/BPO; and (d) Zr12/MPTMS/BPO.

TABLE III
Chemical Shift and Percentage of Si Units, and Degree of Condensation (DOC) of Samples, Calculated by ^{29}Si NMR Spectra Deconvolution

Unit	δ (ppm)	MPTMS/BPO %	MPTMS/H_2O/BPO %	Zr12/MPTMS/BPO %	Zr12/MPTMS/H_2O/BPO %
T^0	−41.5	67.4	0.0	0.0	0.0
T^1	−48.4	13.4	0.0	9.8	0.0
T^2c	−54.2	0.0	9.5	12.8	10.8
T^2	−57.6	10.6	28.1	23.3	43.4
T^3	−65.3	8.6	62.4	54.1	41.5
DOC		20.1	87.5	81.4	81.9

Interestingly, the Zr12/MPTMS/BPO sample had a similar DOC of around 80% with no T^0 and just 10% of T^1, meaning that the Zr oxo-clusters interact with the silane driving the cleavage of the Si-OMe bonds due to the presence of acid sites. This effect had already been noticed in hybrids consisting of VTMS and Zr12, when the DOC of the systems was around 80%,[20] and attributed to the water produced *in situ* by the reaction between the bridging acid molecules bonded to the core of the zirconium oxo-cluster and just the methoxy groups.[20] The presence of Zr oxo-clusters gives rise to a steric hindrance, however, which reduces the possibility of silanol condensation, leaving a certain amount of T^1, T^2 units. The hampering effect of the oxo-cluster could also be inferred for the Zr12/MPTMS/H2O/BPO sample, where there were more T^2 than T^3 units.

Figure 5 shows the ^{29}Si spectra. In addition to the above-mentioned quantitative consideration, it is clear that—in all but the MPTMS/BPO sample—the T^2 peak is not Lorentzian, but composed of at least two components, at −54.3 and −57.8 ppm. They are usually associated with cyclic (T^2c) and linear structures, respectively.[38] This fits perfectly with the FTIR analysis on the samples, which suggested the presence of only ladder-like structures in the MPTMS/BPO sample showing only a small T^2 peak centered at −58 ppm. According to FTIR data, both MPTMS/BPO/H2O and Zr12/MPTMS BPO present a certain amount of cages, cycles, and trimers, which contribute to the T^2c signal at about −54 ppm. The sample Zr/MPTMS/BPO/H_2O shows another peak at −70.7 ppm in the T^3 unit range,[39] that accounts for about 5% of the total and whose interpretation is uncertain.

^{13}C NMR

MPTMS is fully polymerized by the thermal treatment with BPO (Fig. 6) because the peaks corresponding to carbon atoms **1** and **2** (Scheme 1) disappear, giving rise to peaks **1a** and **2a**. As is deducible from the ^{29}Si spectrum, the treatment affects the inorganic head only to a minor extent, due to the persistence of peak **8** (Si-OMe) and the small shift (2 ppm ca.) of peak **7**. Conversely, MPTMS prehydrolysis induces the almost complete disappearance of the methoxy groups linked to Si, and the subsequent condensation is responsible for the reduced mobility of the matrix, as demonstrated by the broadening of all the peaks and the 6 ppm downfield shift of **7**. The polymerization is incomplete because of a minimal presence of **1** at 127.2, **2** at 139.0 ppm, and **4** at 168.9 ppm. The rigidity of the system, demonstrated by the high DOC, probably reduces its polymerization capacity, in much the same way as in the Zr12/MPTMS/H2O/BPO system. The peaks are broad and the methoxy groups are fully hydrolyzed, but polymerization is incomplete. On the other hand, the

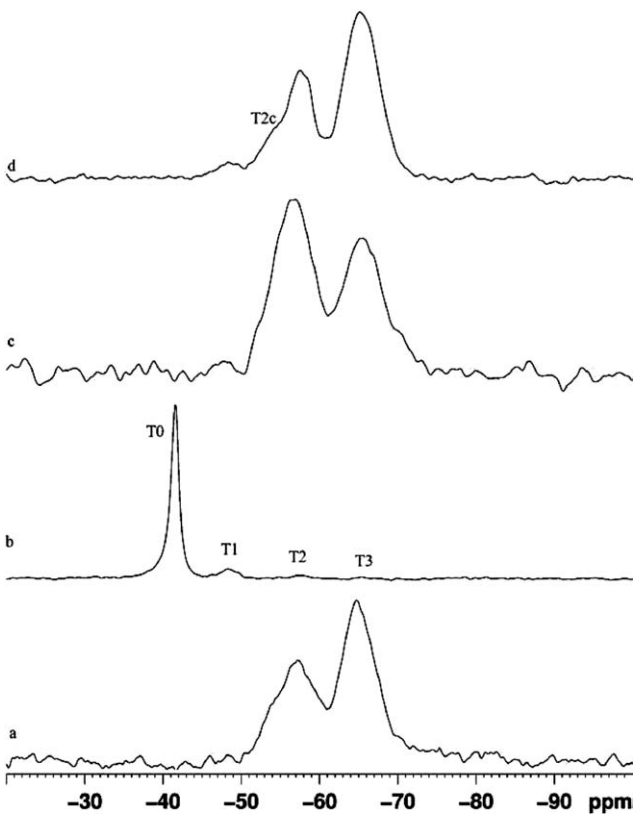

Figure 5 ^{29}Si MAS NMR spectra of: (a) MPTMS/H_2O/BPO; (b) MPTMS/BPO; (c) Zr12/MPTMS/H_2O/BPO; and (d) Zr12/MPTMS/BPO.

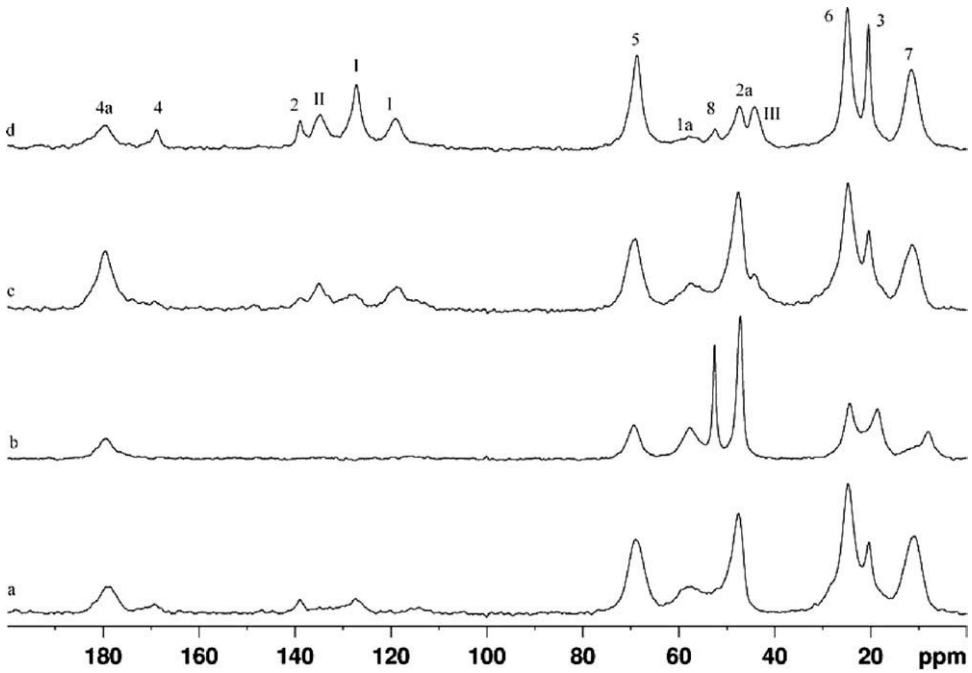

Figure 6 ^{13}C MAS NMR spectra of: (a) MPTMS/H_2O/BPO; (b) MPTMS/BPO; (c) Zr12/MPTMS/H_2O/BPO; and (d) Zr12/MPTMS/BPO.

hybrid that was not prehydrolyzed has a poorly polymerized matrix due to a major presence of peaks **1** and **2**, with some contribution from **1a** and **2a;** this is reflected by the area of peaks **4** and **4a**, which are the carbonyls close to the double bond and the polymerized part, respectively. These two peaks are used to calculate the extent of the samples' polymerization, as shown in Table IV. There is also a residual peak **8**, which confirms a significant but incomplete condensation of the inorganic part. A certain overlapping of the peaks prevents a deep discussion of the oxo-clusters' behavior, which seems here to be almost unaffected by the thermal process, unlike the case of the Zr12/VTMS hybrids,[20] where the VAA partially isomerized and some double bonds were broken.

DISCUSSION

According to eqs. (1)–(3) and Schemes 2–5, free-standing films can be prepared from MPTMS via two processes: hydrolysis–condensation of the methoxy groups (eqs. 1 and 2) followed by polyaddition of the vinylidene groups (Scheme 2), producing a tough hybrid gel and short carbon chains; or radical polymerization of the methacrylate groups (Scheme 2) followed by the hydrolysis–condensation step (eqs. 1 and 2), which produces flexible polymers with a tensile strength that is lower, the longer the carbon chain.[22–24,40–43] The final features of MPTMS-based hybrids thus correlate closely with the nature of the interactions between inorganic network and organic phase depending on the synthesis procedure involved.

In this study we investigated the effect of inorganic condensation on the capacity for radical bulk polymerization of the organic functions, and consequently also on the structural features of the hybrid polymers. The sample prepared from hydrolyzed MPTMS and adding BPO shows a very high DOC (Table III) of the silsesquioxane network, which prevents the formation of long organic chains through radical polymerization (Scheme 2). On the basis of the almost unchanged position of the infrared signal of the carbonyl of the methacrylate groups (Fig. 4), these must not have polymerized completely [Fig. 4(a), Table IV], due to less mobile radical species. Both organic and inorganic moieties in MPTMS/H_2O/BPO sample reacted, leading to a highly condensed bulk material without a detectable amount of

TABLE IV
Yield of MPTMS Polymerization Calculated from Area of Carbonyl Peaks in ^{13}C Spectra (after Subtracting the Contribution of Carbonyl from the Oxo-Cluster Coming into the Same Chemical Shift as 4a)

Signal	Δ (ppm)	MPTMS/BPO	MPTMS/H_2O/BPO	Zr12/MPTMS/BPO	Zr12/MPTMS/H_2O/BPO
4a	179	100.0	81.1	71.1	94.4
4	169	0.0	18.9	28.9	5.6

residual methoxy groups. The hybrid polymer is consequently extremely rigid and brittle.

On the other hand, according to the ^{13}C-NMR results (Table IV), MPTMS/BPO polymerizes completely in a nonhydrolytic environment, and this is confirmed by the reduction of C=C signal intensity and the large C=O shift towards values typical of the polymer PMMA in the FTIR spectrum [Fig. 4(b)].[44] In nonhydrolytic condition, inorganic polycondensation may occur mainly through thermal cleavage (eq. 3), thanks to the heat released by radical polymerization.[32] Thus, very small silica-based domains are formed, as suggested by the low DOC value (Table III). Therefore, MPTMS-derived hybrids, being not exposed to the stresses arising from large inorganic condensation process, undergo little shrinkage and probably form long carbon chains. The alkyl residuals also have a lubricant or plasticizing effect on the macromolecules, making them less brittle and rubbery as shown during the first scan of DMS analysis.

When MPTMS is reacted with Zr12 without BPO, DSC curves bore witness to a radical polymerization of the organic moieties [Fig. 2(a,b)]. Considering that the neat MPTMS is unable to polymerize upon heating and the Zr12 clusters decompose,[20] the interaction between organosilane and Zr oxo-clusters should therefore favor the formation of radical species by thermal activation. This was observed also using VTMS instead of MPTMS [Fig. 2(c,d)]. The Zr oxo-clusters provide metal sites suitable for coordinating the methacryloxy or vinyl groups of the silane, and nucleophilic substitution can initiate polymerization (Scheme 4). It has been reported, in fact, that zirconium alkoxide previously reacted with acetyl acetone could self-initiate the polymerization of 2hydroxyethyl methacrylate (HEMA) through an intermediate anionic species.[26,45]

In the presence of BPO, the DSC traces (Fig. 3) of Zr12/MPTMS/BPO indicate that at least two polymerization processes take place: the main one, at a lower temperature, is due to homo-polymerization of the methacryloxy groups (Scheme 2); the higher-temperature process is mainly attributable to homo- or copolymerization (Scheme 3) of the vinyl groups belonging to Zr12. These groups dependently on being chelating or bridging and by the extent of interaction with the silsesquioxane network, polymerize at different temperature.[20]

The silane prehydrolysis (Zr12/MPTMS/H_2O/BPO) strongly improves the capacity for cyclosiloxane formation (Table III). Indeed, the silsesquioxane network obtained in hydrolytic condition shows a huge number of T^2c units. This is consistent with the higher mass loss on heating by comparison with the one that was not prehydrolyzed. A lower T^3 content generates a mobile network and enables a virtually complete methacrylate polymerization (Table IV).

The DOC value (Table III) is similarly high for both Zr12/MPTMS/BPO and Zr12/MPTMS/H_2O/BPO samples. This implies that MPTMS hydrolysis/condensation takes place even when no water is added, indicating the role of Zr12 in promoting sol–gel reactions for MPTMS. Actually, it had already noted this behavior in VTMS/Zr12/BPO systems, and we suggested that bridging acid molecules bonded to the core of the zirconium oxo-cluster react with the methoxy groups, producing water *in situ*.[20] Besides providing a source of water, this reaction may modify the Zr oxo-clusters to some extent: FTIR analyses are inconclusive on this issue, though the reduction in intensity and the broadening of the bridging acetate FTIR signals point to a change in Zr12 structure (Fig. 4). The involvement of Zr12 in the sol–gel reactions modifies not only the structure of the cluster, but also the propensity of the vinyl acetate groups to be homo- or copolymerized (Schemes 3, 4, and 5a).

The polymerization process can be also promoted by the silanols on the T^2 units, which can interact via hydrogen bond with the methacrylate groups (Schemes 5b and c), this new arrangement facilitates subsequent radical homo-polymerization.[28] Copolymerization may also occur between MPTMS and Zr12, albeit to a lesser extent, and it seems to be more likely in the absence of prehydrolysis because a lower number of silanols form (Scheme 5a). This interpretation is supported by the results of DMS. The two hybrid polymers' behavior differs only in the first scan, when the prehydrolyzed sample shows a T_g value lower than the sample prepared without any prehydrolysis. The latter sample consequently appears less viscous, due to a higher extent of phase interaction between the silsesquioxane and zirconia-rich domains, induced by copolymerization of the methacrylate and vinyl acetate groups. The prehydrolyzed sample has a higher methacrylate polymerization yield (probably due mainly to homo-polymerization) and higher G'' and tan δ values. In the subsequent DMS scans, both samples are involved in thermally activated copolymerization and siloxane condensation, which cause a loss of viscous behavior and make the hybrid materials become similar.

Unlike the case of Zr12/VTMS previously studied,[19,20] all the samples containing MPTMS are rigid and rather brittle, whatever the synthesis conditions.

CONCLUSIONS

This study demonstrates that MPTMS/BPO polymerizes completely if no hydrolysis is carried out, preserving alkoxy residuals, which make the polymer rubbery and sensitive to moisture.

Polymerization of MPTMS and Zr12 occurs through a polyaddition activated by Zr12 without a thermal initiator, whereas a radical process takes place when adding BPO. Both bulk organic polymerization and inorganic polycondensation produce hybrid polymers consisting of organic chains and mixed silicon and zirconium inorganic networks.

This study confirms that a nonhydrolytic environment favors radical homo- and copolymerization of the methacrylate groups, with an extended interaction with the silsesquioxane network, which is formed through the availability of water produced *in situ* thanks to the reaction between Zr12 and alkoxide groups. When the silane is prehydrolyzed, the silsesquioxane network forms extensively with a larger phase separation with the zirconia domains.

The hybrid polymers have high glass transition temperatures, i.e., 140°C and 180°C for the samples with and without prehydrolysis, respectively. The samples retain their shape and size due to the lack of viscous flow after glass transition. Actually, the glass transition disappears when the thermal cycles are repeated.

This study confirms the strong dependence of the physical and mechanical properties of Zr12/MPTMS hybrid materials on the extent of interaction between phases.

References

1. Miller, J. B.; Ko, E. I. J Catal 1996, 159, 58.
2. Soppera, O.; Croutxe'-Barghorn, C.; Carrè, C.; Blanc, D. Appl Surf Sci 2002, 186, 91.
3. Ivanovici, S.; Kickelbick, G. J. Sol-Gel Sci Technol 2008, 46, 273.
4. Djourelov, N.; Suzuki, T.; Misheva, M.; Margac.a, F. M. A.; Miranda Salvado, I. M. J Non-Cryst Sol 2005, 351, 340.
5. Wang, H.; Xu, P.; Zhong, W.; Shen, L.; Du, Q. Polym Degrad Stab 2005, 87, 319.
6. Malenovska, M.; Litschauer, M.; Neouze, M. A.; Schubert, U.; Peled, A.; Lellouche, J. P. J Organomet Chem 2009, 694, 1076.
7. Malenovska, M.; Neouze, M. A.; Schubert, U. Dalton Trans 2008, 34, 4647.
8. Saravanamuttu, K.; Min, D. X.; Najafi, S. I.; Andrews, M. P. Can J Chem 1998, 76, 1717.
9. Park, O. K.; Jung, J. I.; Bae, B. S. J Mater Res 2001, 16, 2143.
10. Armelao, L.; Eisenmenger-Sittner, C.; Groenewolt, M.; Gross, S.; Sada, C.; Schubert, U.; Tondello, E.; Zattin, A. J Mater Chem 2005, 15, 1838.
11. Armelao, L.; Bertagnolli, H.; Gross, S.; Krishnan, V.; Lavrencic-Stangar, U.; Müller, K.; Orel, B.; Srinivasan, G.; Tondello, E.; Zattin, A. J Mater Chem 2005, 15, 1954.
12. Armelao, L.; Gross, S.; Müller, K.; Pace, G.; Tondello, E.; Tsetsgee, O.; Zattin, A. Chem Mater 2006, 18, 6019.
13. Puchberger, M.; Kogler, F. R.; Jupa, M.; Gross, S.; Fric, H.; Kickelbick, G.; Schubert, U. Eur J Inorg Chem 2006, 16, 3283.
14. Gao, Y.; Kogler, F. R.; Schubert, U. J Polym Sci Part A Polym Chem 2005, 43, 6586.
15. Kogler, F. R.; Koch, T.; Peterlink, H.; Seidler, S.; Schubert, U. J Polym Sci Part B: Polym Phys 2007, 45, 2215.
16. Kogler, F. R.; Schubert, U. Polymer 2007, 48, 4990.
17. Kogler, F. R.; Jupa, M.; Puchberger, M.; Schubert, U. J Mater Chem 2004, 14, 3133.
18. Schubert, U. J Sol-Gel Sci Technol 2003, 26, 47.
19. Di Maggio, R.; Dirè, S.; Callone, E.; Girardi, F.; Kickelbick, G. J Sol-Gel Sci Technol 2008, 48, 168.
20. Di Maggio, R.; Dirè, S.; Callone, E.; Girardi. F.; Kickelbick, G. Polymer 2010, 51, 832.
21. Girardi, F.; Graziola, F.; Aldighieri, P.; Fedrizzi, L.; Gross, S.; Di Maggio, R. Prog Org Coat 2008, 62, 376.
22. Abe, Y.; Honda, Y.; Gunij, T. Appl Organomet Chem 1998, 12, 749.
23. Gunji, T.; Makabe, Y.; Takamura, N.; Abe, Y. Appl Organomet Chem 2001, 15, 683.
24. Gunji, T.; Kawaguchi, Y.; Okonogi, H.; Sakan, T.; Arimitsu, K.; Abe, Y. J Sol–Gel Sci Technol 2005, 33, 9.
25. Maggini, S; Girardi, F.; Mueller, K; Di Maggio, R. J Appl Polym Sci, DOI: 10.1002/app.35217.
26. Di Maggio, R.; Fambri, L.; Cesconi, M.; Vaona, W. Macromolecules 2002, 35, 5342.
27. Dirè, S.; Tagliazucca, V.; Brusatin, G.; Bottazzo, J.; Fortunati, I.; Signorini, R.; Dainese, T.; Andraud, C.; Trombetta, M.; Di Vona, M. L.; Licoccia, S. J Sol-Gel Sci Technol 2008, 48, 217.
28. Zhou, H.; Li, Q.; Lee, T. Y.; Guymon, C. A.; Jönsson, E. S.; Hoyle, C. E. Macromolecules 2006, 39, 8269.
29. Chen, L. F.; Cai, Z. H.; Zhou, W.; Lan, L.; Chen, X. J. J Mater Sci 2005, 40, 3497.
30. Garnweitner, G.; Niederberger, M. J Am Ceram Soc 2006, 89, 1801.
31. Di Maggio, R.; Campostrini, R.; Guella, G. Chem Mater 1998, 10, 3839.
32. Kickelbick, G. J Sol-Gel Sci Technol 2008, 46, 281.
33. Orel, B.; Ješe, R.; Vilčnik, A.; Lavrenčič Štangar, U. J Sol-Gel Sci Technol 2005, 34, 251.
34. Voronkov, M.; Lavrentyev, V. I. Top Curr Chem 1982, 102, 199.
35. Brown, J. F.; Vogt, L. H. J Am Chem Soc 1965, 87, 4313.
36. Yoshino, H.; Kamiya, K.; Nasu, H. J Non Cryst Solids 1990, 126, 68.
37. Oubaha, M.; Dubois, M.; Murphy, B.; Etienne, P. J Sol-Gel Sci Technol 2006, 38, 111.
38. Feuillade, M.; Croutxè-Barghorn, C.; Carrè, C. Prog Solid State Chem 2006, 34, 87.
39. Engelhardt, M.; Jancke, H. Polymer Bull 1981, 5, 577.
40. Nishiyama, N.; Horie, K.; Asakura, T. J Appl Polym Sci 1987, 34, 1619.
41. Delattre, L.; Dupuy, C.; Babonneau, F. J Sol-Gel Sci Technol 1994, 2, 185.
42. O'Shea, M. S.; George, G. A. Polymer 1994, 35, 4181.
43. Mai, C.; Cornu, J. F.; Arnaud, L.; Perez, J. J Sol-Gel Sci Technol 1994, 2, 135.
44. Huang, Z. H.; Qiu, K. Y. Polymer 1997, 38, 521.
45. Versace, D.; Soppera, O.; Lavelée, J.; Croutxé-Barghorn, C. New J Chem 2008, 32, 2270.